

Photoalignment in Ultrathin Films of a Layer-by-Layer Deposited Water-Soluble Azobenzene Dye

Rigoberto Advincula,^{*,†,‡} Mi-Kyoung Park,^{†,‡} Akira Baba,^{§,||} and Futao Kaneko[§]

Department of Chemistry, University of Houston, Houston, Texas 77204-5003, Department of Chemistry, University of Alabama at Birmingham, Birmingham, Alabama 35294-1240, and Department of Electrical and Electronic Engineering, Niigata University, Ikarashi 2-8050, Niigata 950-21, Japan

Received April 17, 2002. In Final Form: November 8, 2002

The photoalignment of alternate layer-by-layer (LBL) deposited water-soluble azobenzene dye, direct red 80 (DR80), and polycations have been investigated. The ultrathin films were probed by polarized irradiation, UV-vis spectroscopy, and angle-dependent optical retardation measurements using a hybrid liquid crystal (LC) cell. Dye aggregates within layers were found to reorient anisotropically with polarized irradiated visible light. The selective photoisomerization process primarily enhances the *E*-isomer, giving high dichroism with the long axes of the azobenzene dye oriented perpendicular to the polarization vector of irradiated light (actinic light). The degree of photoalignment was dependent on the number of adsorbed layers, aggregation behavior, and type of polycation pairs in contrast to spin-coated or Langmuir-Blodgett (LB) films. Atomic force microscopy (AFM) before and after photoisomerization showed lateral expansion of the morphological features consistent with greater anisotropic ordering. These results correlated with the *in-plane* azimuthal LC photoalignment behavior in hybrid LC cells. Interesting trends were observed, including thickness-dependent photoalignment behavior, different irradiation stabilities, phase shift, and read-write capabilities as photoactive ultrathin films.

Introduction

Photochromic materials, whose optical properties can be varied reversibly by light, have enormous potential for electrooptical and optical devices.¹ Applications include the following: liquid crystal (LC) displays, holographic surface relief gratings, optical data storage media, etc. Azobenzene derivatives have been widely investigated because of their well-defined reversible *trans*-*cis* or *E*-*Z* photoisomerization property.² Ultrathin films containing these moieties are excellent materials for photocontrol of surface and bulk properties. Using linearly polarized light, these materials can induce; *in-plane* anisotropy in films, surface photoregulation of LC alignment, linear photopolymerization, and anisotropic photobleaching. By employing polymer matrixes, the *Weigert effect*³ has been demonstrated, where polarized reorientation of chromophore dyes result in high optical anisotropies. The photochromic moieties are incorporated by physical blending and covalent tethering.⁴ However, it is not widely known how the nature and morphology of a polymer influences both photo- and thermochromism of a chromophore.⁵ The effect of the matrix on photochromism is not often investigated. There is no complete theory to explain how a photochromic process is linked to matrix

properties.⁶ For practical reasons, spin-coated films of azobenzene materials have been widely used to prepare films for investigating optical properties.⁷ Understanding aggregation and phase behavior of dyes in these blend films can be complicated but is important for understanding optical behavior.

The Langmuir-Blodgett (LB) technique can be used to prepare *oriented* monolayer and multilayer films compared to isotropic spin cast films.⁸ These films allow the fundamental study of physical and chemical properties, such as phase transitions, aggregation, photochemistry, etc., at a *monomolecular* layer level. However, the deposition is tedious and is not adaptable for large-scale processing both in quantity and dimension suitable for commercial applications. Also, the orientation parameters in LB films are known to suppress selective photoalignment because of steric factors on the oriented azobenzene groups.⁹ Self-assembled monolayers (SAMs) of azobenzene groups have also been investigated.¹⁰ A large number of azobenzene systems investigated as SAM and LB films, have been reported.^{2,11}

Recently, there has been great interest for molecularly organized ultrathin films prepared using the alternate

(6) Williams, J.; Daly, R. *Prog. Polym. Sci.* **1977**, *5*, 61.

(7) (a) Ichimura, K.; Suzuki, Y.; Seki, T.; Kawanishi, Y.; Aoki, K., *Makromol. Chem. Rapid Commun.* **1989**, *10*, 5. (b) Ichimura, K.; Seki, T.; Kawanishi, Y.; Suzuki, Y.; Sakuragi, M.; Tamaki, T. In *Photoreactive Materials for Ultrahigh-Density Optical Memory*; Irie, M., Ed.; Elsevier Science: Amsterdam, 1994.

(8) Ulman, A. *An Introduction to Ultrathin Organic Films: From Langmuir-Blodgett to Self-Assembly*; Academic Press: Boston, 1991.

(9) (a) Katayama, N.; Ozaki, Y.; Seki, T.; Tamaki, T.; Iriyama, K. *Langmuir* **1994**, *10*, 1898. (b) Seki, T.; Sakuragi, M.; Kawanishi, Y.; Suzuki, Y.; Tamaki, T.; Fukuda, R.; Ichimura, K. *Langmuir* **1993**, *9*, 211.

(10) (a) Ichimura, K.; Hayashi, Y.; Akiyama, H.; Ikeda, T.; Ishizuki, N. *Appl. Phys. Lett.* **1993**, *63*, 449. (b) Sekkat, Z.; Wood, J.; Knoll, W. *J. Phys. Chem.* **1995**, *99*, 17226. (c) Ichimura, K.; Hayashi, Y.; Akiyama, H.; Ishizuki, N. *Langmuir* **1993**, *9*, 3298.

(11) (a) Ichimura, K.; Hayashi, Y.; Ishizuki, N. *Chem. Lett.* **1992**, 1063. (b) Ichimura, K.; Akiyama, H.; Kudo, K.; Ishizuki, N.; Yamamura, S. *Liq. Cryst.* **1996**, *20*, 423.

* To whom correspondence should be addressed.

† University of Alabama at Birmingham.

‡ University of Houston.

§ Niigata University.

|| Current address: Max Planck Institute for Polymer Research, Mainz D-55021, Germany.

(1) Ichimura, K. *Polymers as Electrooptical and Photooptical Active Media*; Shibaev, V., Ed.; Springer: Berlin, 1996; p 138.

(2) Ichimura, K. *Chem. Rev.* **2000**, *100*, 1847.

(3) Weigert, F. *Naturwissenschaften* **1921**, *29*, 583.

(4) (a) Ho, M.; Natansohn, A.; Ronchon, P. *Macromolecules* **1996**, *29*, 44. (b) Taniike, K.; Matsumoto, T.; Sato, T.; Ozaki, Y.; Nakashima, K.; Iriyama, K. *J. Phys. Chem.* **1996**, *100*, 15508.

(5) Ichimura, K. In *Photochromic and Thermochromic Compounds*; Crano, J. C., Guglielmetti, R., Eds.; Kluwer Academic/Plenum: New York, 1999; Vol. 2, p 9.

layer-by-layer (LBL) adsorption of polyelectrolytes or electrostatic self-assembly (ESA).^{12,15} Alternate deposition is achieved by overcompensation of polyelectrolytes adsorbing on oppositely charged surfaces. The advantages compared to the LB method include the following: It is a simpler technique involving simple equipment and preparation and can be applied to larger substrate dimensions. A large variety of water-soluble macroions or polyions can be used. The individual layers can have distinct molecular thicknesses and ordering.¹³ And last, surfaces of other geometries and colloidal particles can be coated.¹⁴ By using low-molecular-weight species (dyes, bolaform amphiphiles, nanoparticles, etc.), this method has proven more versatile for preparing organized ultrathin films. Thus, incorporating azobenzene dye aggregates into LBL films is attractive.¹⁵ Several groups have demonstrated this concept.¹⁶ Others have reported small-molecule dye-containing LBL assemblies for various optical and sensor applications.¹⁷ The main advantage over spin coating is that the concentration and layer sequence of the dye aggregates can be well-characterized prior to optical studies. In addition, the technique allows the use of polyelectrolytes as a class of polymers for ultrathin film preparation, with material combinations not possible for spin coating. We have recently investigated in detail the preparation of LBL films of water-soluble azobenzene dye derivatives and polycations.¹⁸ It is important to examine in detail the behavior of charged small-molecule dyes in LBL assembly. Azobenzene dyes have long been used as colorants, stains, and markers.¹⁹ In particular, it is important to correlate the dimension, charge density, solubility, nature of aggregation, etc., of these molecular species with photochemical activity.

In this paper, we report the LBL fabrication and photoinduced alignment (photoalignment) of molecularly ordered ultrathin films of a small-molecule azobenzene dye (DR80) and polycations.^{18,20} This molecular chromophoric dye was chosen to have sufficient charge density, photoisomerizability, and high aspect ratio for the *E*-isomer. The molecular assembly process was previously investigated using surface sensitive techniques such as quartz crystal microbalance (QCM), ellipsometry, UV-vis spectroscopy, X-ray reflectometry, and surface plasmon spectroscopy.²¹ Photoalignment studies showed high anisotropies after irradiation with linear polarized visible light.²² Correlation was made on layer ordering, dye

aggregation, and topological domain structures to their photoalignment properties. Comparison was then made with spin-coated films. To better understand their *in-plane* photoalignment behavior, optical retardation in hybrid LC cells was observed as a function of polarizer-analyzer angle (polarimetry).^{9,28} In-plane selectivity of the photoisomerization process was associated with the aggregation nature of the domains resulting in reorientation of the LC molecules. Interesting trends include thickness-dependent behavior, different irradiation stabilities, phase shift, and read-write capabilities as photoactive ultrathin films. The behavior is different from previously reported photoalignment behavior in LB monolayers, SAMs, and spin-coated films.^{7,9-11}

Experimental Section

Materials. The water-soluble anionic (sulfonated) azobenzene dye direct red 80 (DR80) or Sirius red, MW = 1373.09, λ_{\max} = 528 nm, was obtained from Aldrich Chemicals and handled using proper safety procedures.²³ Purification involved recrystallization using solvent mixtures with dimethylformamide (DMF) and ethanol, followed by extensive cold solvent washing. Purity was followed by thin-layer chromatography. The structure of the dye is shown in Figure 1. The molecular dimension of the dye DR80 (Chem 3D software) is 3.4 nm \times 0.8 nm assuming an all-trans or *E*-isomer configuration. Poly(diallyldimethylammonium chloride) (PDDA; MW = 100 000), poly(ethyleneimine) (PEI; MW = 70 000), poly(allylamine hydrochloride) (PAH; MW = 50 000–65 000), and poly(sodium 4-styrenesulfonate) (PSS; MW = 70 000) were commercially obtained from Aldrich and used without further purification. Filtered aqueous solutions (Milli-Q water with 18.2 M Ω resistivity) were prepared with a concentration of 0.001 or 0.001 M/(repeat unit) at pH = 6.5. The borosilicate glass slides (25 mm \times 40 mm \times 0.5 mm) were used as substrates for UV-visible spectroscopy, while Si wafers were used for ellipsometry. The substrates were cleaned by preliminary washing, Piranha solution treatment, and were functionalized immediately with (3-aminopropyl)triethoxysilane (Aldrich, 0.1% in acetone) by SAM procedure.²⁴ The quality of deposition for thicker films was also improved by the initial deposition of three pair-layers of PDDA and PSS.

Layer-by-Layer Deposition. The electrostatic LBL deposition on substrates was done using well-reported procedures.^{12a} The automated dye-polycation deposition was carried out using a HMS series programmable slide stainer apparatus (Carl Zeiss, Inc). In general, the sequence alternated between the oppositely charged dye and polyelectrolyte solutions. Immersion time in each solution was 15 min,²⁵ followed by 2-min immersion in deionized water and then 1 min in a bath with flowing deionized water. This cycle was repeated until the desired number of pair-layers was obtained. DR80 layers were always deposited last. Using this procedure, for example, up to 100 pair-layers were deposited for the DR80/PDDA films.

Instruments. UV-vis spectra were obtained with a Perkin-Elmer Lambda 20 spectrophotometer equipped with a polarized

(12) (a) Decher, G. In *Comprehensive Supramolecular Chemistry*; Sauvage, J. P., Hosseini, M. W., Eds.; Pergamon Press: Oxford, U.K., 1996; Vol. 9, p 507. (b) Bertrand, P.; Jonas, A.; Laschewsky, A.; Legras, R. *Macromol. Rapid. Commun.* **2000**, *21*, 319. (c) Decher, G.; Hong, J. *Makromol. Chem. Macromol. Symp.* **1991**, *46*, 321.

(13) (a) Korneev, D.; Lvov, Y.; Decher, G.; Schmitt, J.; Yaradaikin, S. *Physica B* **1995**, *213/214*, 954. (b) Kellogg, G.; Mayes, A.; Stockton, W.; Ferreira, M.; Rubner, M.; Satija, S. *Langmuir* **1996**, *12*, 5109.

(14) (a) Caruso, F.; Donath, E.; Möhwald, H., *J. Phys. Chem. B* **1998**, *102*, 2011. (b) Donath, E.; Sukhorukov, G. B.; Caruso, F.; Davis, S. A.; Möhwald, H. *Angew. Chem., Int. Ed.* **1998**, *37*, 2201.

(15) Advincula, R. Polyelectrolyte Layer-by-Layer Self-Assembled Multilayers Containing Azobenzene Dye Groups, a review chapter. In *Handbook of Polyelectrolytes and Their Applications*; Tripathy, S. K., Kumar, J., Nalwa, H. S., Eds.; American Scientific: Stevenson Ranch, CA, 2002; Vol. 1, p 65.

(16) (a) Ariga, K.; Lvov, Y.; Kunitake, T. *J. Am. Chem. Soc.* **1997**, *119*, 2224. (b) Cooper, T.; Campbell, A.; Crane, R. *Langmuir* **1995**, *11*, 2713. (c) Yoo, D.; Wu, A.; Lee, J.; Rubner, M. *Synth. Met.* **1997**, *85*, 1425.

(17) (a) He, J.; Bian, S.; Li, L.; Kumar, J.; Tripathy, S. *Appl. Phys. Lett.* **2000**, *76*, 3233. (b) Kometani, N.; Nakajima, H.; Asami, K.; Yonezawa, Y.; Kajimoto, O. *J. Phys. Chem.* **2000**, *104*, 9630.

(18) Advincula, R.; Fells, E.; Park, M. *Chem. Mater.* **2001**, *13*, 2870.

(19) Herbst, W.; Hunger, K. *Industrial Organic Pigments*; VCH Verlagsgesellschaft: Weinheim, Germany, 1997.

(20) (a) Advincula, R.; Fells, E.; Jones, N.; Guzman, J.; Baba, A.; Kaneko, F. *Polym. Prepr. (Am. Chem. Soc., Div. Polym. Chem.)* **1999**, *40*, 443. (b) Advincula, R.; Park, M.; Baba, A.; Kaneko, F. *Polym. Mater. Sci. Eng. (Am. Chem. Soc. Div.)* **1999**, *81*, 77.

(21) (a) Advincula, R.; Inaoka, S.; Roitman, D.; Frank, C.; Knoll, W.; Baba, A.; Kaneko, F. Flat Panel Displays and Sensors—Principles, Materials, and Process; In *MRS Proceedings*; Chalamala, B., Friend, R., Jackson, T., Libsch, F., Eds.; Materials Research Society: Pittsburgh, PA, 2000, 558, 415. (b) Advincula, R.; Kaneko, F.; Baba, A. Liquid Crystal Materials and Development. In *MRS Proceedings*; Spring 1999; Bunning, T., Chien, L. C., Kajiyama, T., Koide, N., Lien, S., Eds.; Materials Research Society: Pittsburgh, PA, 1999; Vol. 559, p 195.

(22) Baba, A.; Kaneko, F.; Shinbo, S.; Kato, K.; Kobayashi, S.; R. Advincula, R. *Mol. Cryst. Liq. Cryst.* **2000**, *347*, 259.

(23) Möller, P.; Wallin, H. *Mutat. Res.* **2000**, *462*, 13.

(24) Fadeev, A.; McCarthy, T. *Langmuir* **2000**, *16*, 7268.

(25) Advincula, R.; Baba, A.; Kaneko, F. *Polym. Mater. Sci. Eng. (Am. Chem. Soc. Div.)* **1999**, *81*, 95.

(26) Hong, J.; Park, E.; Park, A. *Langmuir* **1999**, *15*, 6515.

(27) Sutandar, P.; Ahn, D.; Franses, E. *Thin Solid Films* **1995**, *263*, 134.

(28) (a) Ichimura, K.; Suzuki, Y.; Seki, T.; Hosoki, A.; Aoki, K. *Langmuir* **1988**, *4*, 1214. (b) Seki, T.; Sukuragi, M.; Kawanishi, Y.; Suzuki, Y.; Tamaki, T.; Fukuda, R.; Ichimura, K. *Langmuir* **1993**, *9*, 211.

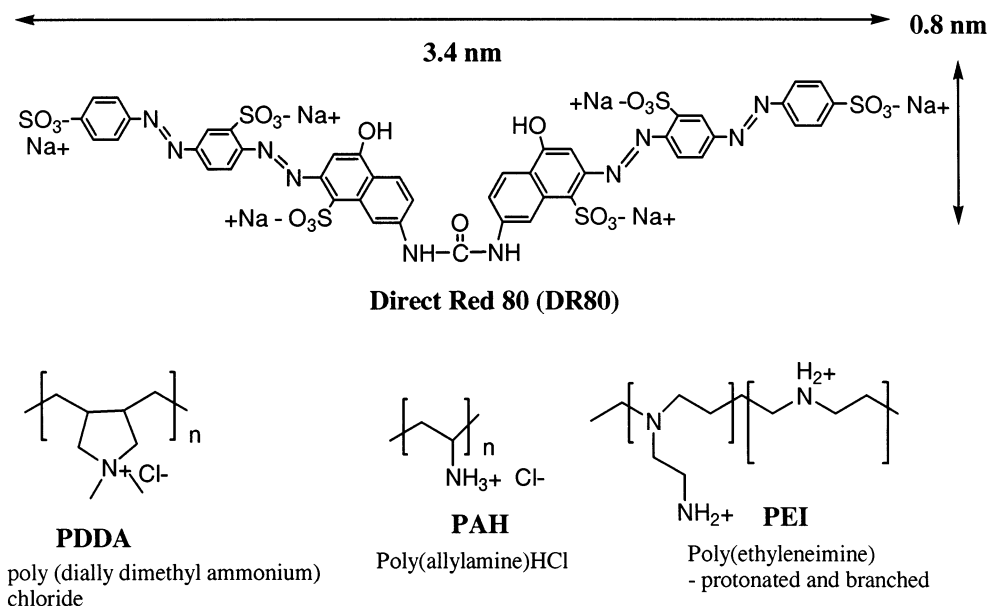


Figure 1. Chemical structure of the direct red 80 dye and polycations used. The molecular dimension of the dye *E*-isomer is also shown.

spectroscopy setup. Ellipsometry was performed using a Multiskop (Optrel, GmbH, Germany) ellipsometer with 632.8 nm He–Ne laser beam at 70° incidence. Both δ and φ values and thickness data (average of three points) were measured and calculated using a refractive index of 1.5.²⁶ Surface morphology were obtained by atomic force microscopy (AFM) under ambient conditions (22–23 °C, 40% relative humidity) using a PicoScan system (Molecular Imaging) equipped with an $8 \times 8 \mu\text{m}$ scanner. The magnetic AC (MAC) mode was used for all the AFM images. A MAC lever, silicon nitride, Si_3N_4 , based cantilever coated with magnetic film, was used as AFM tip. The force constant of the tip from the triangular-shaped cantilever was 0.1 N/m, and the resonance frequency is ~ 100 kHz. The force between the tip and the sample was typically 1 nN. Besides the raw image, a Fourier-filtered phase image was obtained to emphasize the periodic features. The fast Fourier transform (FFT) program was supplied by Molecular Imaging. A 500-scan accumulation was used for an acceptable signal/noise ratio.

Photoirradiation and Polarized UV–Vis Spectroscopy. Unpolarized and polarized UV and visible irradiation was done using a 150 W Xe arc lamp with a beam expanding lens, employing band-pass filters to obtain $\lambda > 430$ nm for the enhanced *E*-isomer photoisomerization. The irradiation intensity based on the distance, area, and intensity of the lamp was calculated to be 190 mW/cm². A dichroic sheet polarizer was set between the lamp and sample to obtain a desired polarized UV irradiation with a reduced intensity of 50 mW/cm². Isotropy of the films was checked by UV–vis spectroscopy before each experiment. The $\theta = 0^\circ$ axis is defined to be parallel to the longer side of the rectangular glass substrate (40×25 mm). When polarized irradiation is introduced normal to the substrate plane, a polarization direction either parallel ($\theta = 0^\circ$ or A_{\parallel}) or perpendicular ($\theta = 90^\circ$ or A_{\perp}) can be assigned with respect to polarized UV–vis spectroscopy. The spectrum is then expected to show different absorption intensities at angles associated with a specific irradiation direction. The presence of dichroic features (birefringence) indicates anisotropic molecular projections of the absorbing species on the film. By definition, the dichroic ratio is the ratio of peak intensity for s-polarized incident light to that of p-polarized light and is given by the following equation:²⁷ $\text{DR} = (A_{\perp} - A_{\parallel}) / (A_{\perp} + A_{\parallel})$. Alternatively, the equation relating the degree of ordering by the orientation parameter (S) of the dyes can also be used, where $S = (A_{\parallel} - A_{\perp}) / (A_{\parallel} + 2A_{\perp})$.²⁶

Hybrid LC Cell Fabrication and Investigations. A hybrid LC cell was fabricated with the DR80/polycation substrate and a glass substrate modified with an LB monolayer of stearic acid.²⁸ This was done by sandwiching the nematic LC (4-pentyl-4'-cyanobiphenyl) (N–35 °C–I) or (5CB) material between the

modified substrates and separated by a Mylar spacer (16 μm). A homeotropic alignment was induced from the stearic acid side of the cell (Figure 2). The optical retardation was monitored by a photodetector following the intensity of transmitted linearly polarized He–Ne laser (632.8 nm, 5 mW) through the cell and a polarizer/analyzer as a function of the rotation angle (ϕ) of the cell. The experimental setup has been previously reported.^{28,40} The transmittance intensity was observed with a fixed analyzer position while the hybrid LC cell was rotated. The results are best plotted in a polar plot where the transmittance intensity axis extends from the center of the circle (radius), and the rotation angle (ϕ) is defined by the circumference of the circle. This can also be plotted alternatively in an X–Y (ϕ vs intensity) scatter plot.

Results and Discussion

Multilayer LBL Film Formation and Dye Aggregation. UV–vis spectroscopy and ellipsometry verified the LBL self-assembly process of the dye/polycation layers and their aggregation behavior.¹⁸ The films prepared were clear, transparent, and uniform, with good optical quality as seen by the naked eye. UV–vis spectra for the DR80/

(29) Lambert, J. *Organic Structural Spectroscopy*; Prentice Hall: Upper Saddle River, NJ, 1998.

(30) (a) McRae, E.; Kasha, M. *J. Phys. Chem.* **1958**, *28*, 721. (b) Okahata, Y.; Kunitake, T. *J. Am. Chem. Soc.* **1979**, *101*, 5231.

(31) (a) Dante, S.; Advincula, R. Frank, C.; Stroeve, P. *Langmuir* **1999**, *15*, 193. (b) Suzuki, I.; Ishizaki, T.; Hoshi, T.; Anzai, J. *Macromolecules* **2002**, *35*, 577.

(32) Cimrova, V.; Neher, D.; Kostromine, S.; Bieringer, Th. *Macromolecules* **1999**, *32*, 8496.

(33) Han, M.; Ichimura, K. *Macromolecules* **2001**, *34*, 90.

(34) Schönhoff, M.; Mertesdorf, M.; Losche, M. *J. Phys. Chem.* **1996**, *100*, 7558.

(35) Gibbons, W.; Shannon, P.; Sun, S.; Swetlin, B. *Nature* **1991**, *351*, 49.

(36) Han, M.; Morino, S.; Ichimura, K. *Macromolecules* **2000**, *33*, 6360.

(37) Fritzl, A.; Schonhals, A.; Sapich, B.; Stumpe, J. *Macromol. Chem. Phys.* **1999**, *200*, 2213.

(38) (a) Wang, R.; Jiang, L.; Iyoda, T.; Tryk, D.; Hashimoto, K.; Fujishima, A. *Langmuir* **1996**, *12*, 2052. (b) Seki, T.; Kojima, J.; Ichimura, K. *Macromolecules* **2000**, *33*, 2709.

(39) Garnaes, J.; Schwartz, D. K.; Viswanathan, R.; Zasadzinski, J. A. N. *Nature* **1992**, *357*, 54.

(40) Advincula, R.; Park, M. K. In-Plane Photoalignment of Liquid Crystals by Azobenzene Polyelectrolyte Layer-by-Layer Ultrathin Films. *Langmuir*, in press.

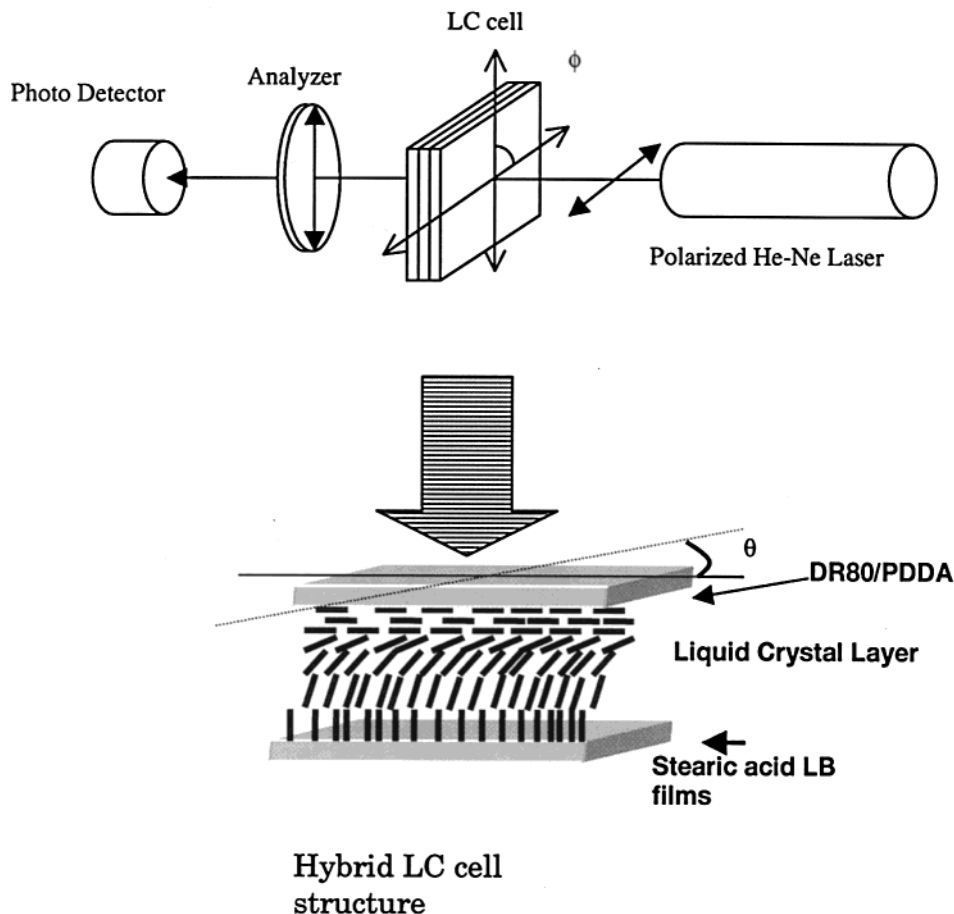


Figure 2. Hybrid LC cell setup was used to observe optical retardation of photoalignment. The rotation angle (ϕ) is defined by rotation of the cell, and the intensity of transmission was monitored through a fixed analyzer.

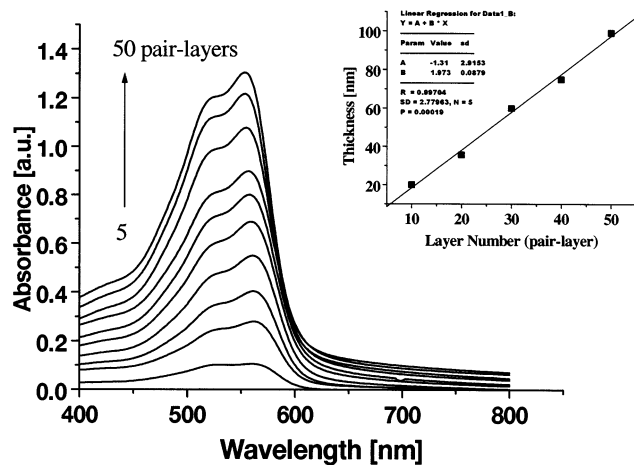


Figure 3. UV-vis spectra as a function of layer number showing increasing dye concentration. The change in thickness as obtained by ellipsometry is also shown (inset). Reprinted with permission from ref 18. Copyright 2001 American Chemical Society.

PDDA multilayers taken as a function of increasing layer numbers are shown in Figure 3.¹⁸ The absorbance increased linearly with the number of dye-polymer pair-layers. The λ_{\max} centered at 562 nm is attributed to the $\pi-\pi^*$ transition for the dye. DR80 has four azobenzene groups with a conjugation length consistent with the high molar absorptivity, $\epsilon_{\max} = 4.2 \times 10^4 \text{ M}^{-1} \text{ cm}^{-1}$ observed in aqueous solutions. Typical values for a single azobenzene in isoctane are $\epsilon_{\max} = 2.26 \times 10^4 \text{ M}^{-1} \text{ cm}^{-1}$ and $\lambda_{\max} = 318 \text{ nm}$ for a trans configuration.²⁹

The LBL film absorbance was strongly red-shifted: 34 nm compared to the $1 \times 10^{-5} \text{ M}$ solution ($\lambda_{\max} = 528$) and 38 nm with PDDA present ($\lambda_{\max} = 524 \text{ nm}$) in solution indicating aggregates in the film. It should be noted that the aggregation of dye molecules in ordered structures with corresponding dipoles results in a splitting of the excitation energy levels.³⁰ As a consequence, shifts in the absorption spectra are observed, depending on the mutual orientation of the interacting dipole moments. When the dipole moments are parallel, a hypsochromic (blue) shift H-aggregation (H band) occurs. If the transition dipoles are in-line, rather than parallel, the spectra exhibit a bathochromic (red) shift and the aggregates are termed J-aggregates (J-band). The red-shift behavior for DR80/PDDA indicates the formation of J-aggregates in each layer where the orientation of the dye aggregates can be described as tilted.¹⁸ Similar aggregation behavior has been observed by Kunitake on a variety of water-soluble dyes.^{16a} Comparison of the λ_{\max} values with increasing number of layers reveal a small shift in λ_{\max} position occurring intermittently, indicating that the degree of aggregation changes with thickness. This behavior has been previously observed for azobenzene LBL films and is influenced by the packing order achieved after the addition of each layer.^{18,31} The reorganization of the aggregates with increasing layer thickness is consistent with a self-healing capacity for these types of films.¹²

The average thickness per dye-polycation pair-layer was determined to be $1.9 \pm 0.1 \text{ nm}$ with an absorbance of 0.032 au/pair-layer, i.e., an average absorbance/thickness value of 0.017 au/nm. It has also been previously reported that salts can increase the density of dyes

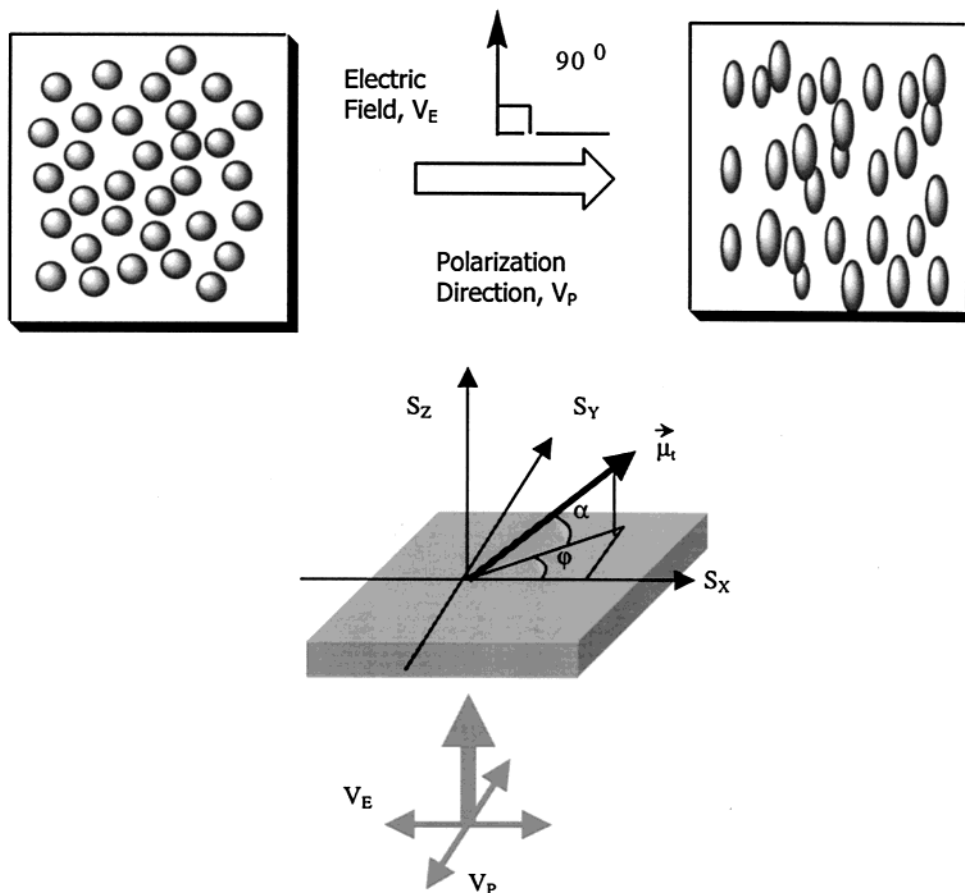


Figure 4. Photoalignment scheme showing how initially isotropic dye aggregates (shown as circles) can be made anisotropic by the use of linearly polarized light resulting in reorientation and change in shape. The order and orientation parameters are also defined with irradiation (see discussions).

adsorbed per pair-layer.¹⁸ The DR80 dye–polycation layer-by-layer assembly process has been investigated by a number of other surface sensitive techniques, including quartz crystal microbalance (QCM), X-ray reflectometry, and surface plasmon spectroscopy.^{20,21} Results have always shown that the deposition is consistently linear and the dyes are ordered as aggregated domains in each layer.¹⁸ Note that the term layer ordering does not necessarily refer to distinct layers with a finite boundary but rather a consequence of alternately adsorbed layers of two different and oppositely charged polyelectrolyte species.¹² No Bragg peaks are expected even by X-ray diffraction since there is no sufficiently distinct electron density profile between layers.^{20,21} Interpenetration of the adjacent layers cannot be ruled out, but should be limited by surface coverage, film equilibrium, substrate defects, and thickness of the oppositely adsorbing species. However, the fact that a linear absorbance and thickness increase were observed for each deposition cycle indicates a quantified adsorption of dyes aggregated as layers. Much discussion has been covered on this topic in several review articles¹² and on similar dye–polyelectrolyte systems.¹⁶ In summary, the characterization of these present DR80 films indicate a uniformly prepared LBL multilayer suitable for photoisomerization and photoalignment studies.

In-Plane Selective Photoisomerization or Photoalignment. A review of the photoalignment process in azobenzenes is as follows:² The photoalignment can be induced in-plane (film surface plane or S_x and S_y) by a selective and reversible photoconversion process utilizing polarized UV or visible irradiation (Figure 4). Initially, the azobenzene chromophores are isotropic ($S_0 = S_x = S_y$

$= S_z$) in orientation. Upon polarized light irradiation with vectorial electric field, V_E , and polarization, V_P , the highest absorbance is expected where the transition dipole moment (oscillator strength), μ_t , of the conjugated azobenzene group is the strongest, i.e., parallel to the molecular long axis of the trans or *E*-isomer.²⁸ In the presence of linearly polarized light, photons are absorbed by the azobenzene molecules according to $\cos^2 \varphi$, where φ is the angle between the azobenzene μ_t and V_E of irradiated light. The absorbing azobenzene groups will undergo photoisomerization trans–cis–trans or *E–Z–E* resulting in photostationary states of azobenzenes where the transition dipole moment, μ_t , becomes parallel to the polarization vector, V_E (in this case set parallel to S_y).³² The result is a uniaxial reorientation of the azobenzene transition dipole into the direction perpendicular to polarization vector, V_P , of incident light with the dipole momentum equal to zero.³³ Note that azobenzene groups can also be aligned out-of-plane or along S_z , by the angle, α , which can also result in a depletion of the oriented in-plane photostationary states and its contribution to absorbance.³⁴

The photoalignment can also be explained in terms of the selective excitation of azobenzene molecular dye excited states.²⁸ By selectively exciting with UV light, only the *Z*-form rich photostationary state for π – π^* transition is obtained. This is a typical *E–Z* photoisomerization experiment. However, upon exposure *only* to filtered visible light, the high aspect ratio *E*-isomer with the n – π^* transition is the major component of the photostationary states.²⁸ This means that no decay of the azobenzene *E*-isomer is realized, if subjected only to visible light irradiation for the n – π^* transition. Changing the polar-

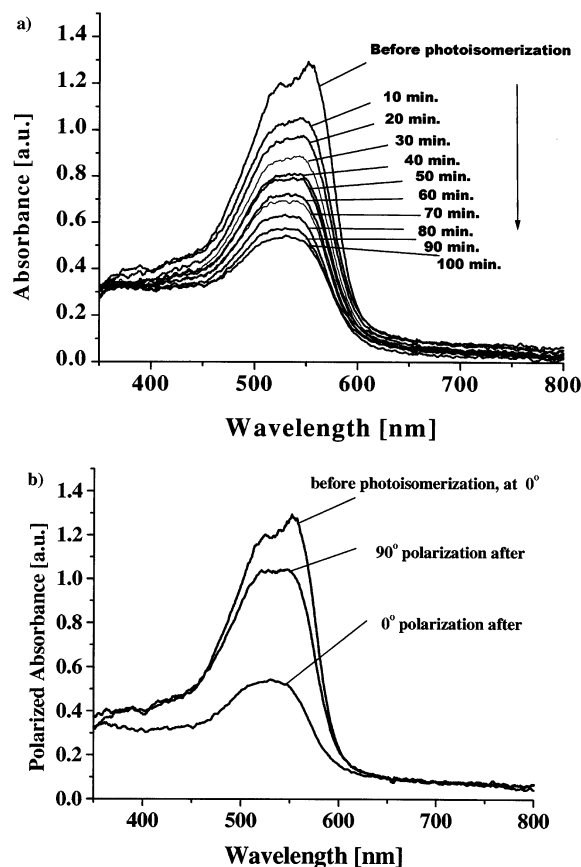


Figure 5. Polarized UV-vis spectra of a 50-layer DR80/PDADMAC film: (a) change in absorbance with irradiation time $\theta = 0^\circ$ and (b) substrate rotated 90° or perpendicular to polarization of irradiated light, showing high dichroism. Reprinted with permission from ref 18. Copyright 2001 American Chemical Society.

ization vector, \mathbf{V}_E , or polarization = θ of the linear polarized light causes reorientation of the rodlike *E*-isomer acting as a "molecular rotor". This generates a large birefringence, especially on the dielectric constants since the dye molecular long axis becomes reoriented. This photoselective orientation is the basis for the *Weigert effect*.³ Note that both nondestructive and destructive photoorientation (in the case of a photochemical reaction) can give the Weigert effect. An alternative photoorientation mechanism has been suggested involving thermal dissipation of the electronic excitation energy in oriented aggregates.³⁴

Previous work on spin-coated films of azobenzene dyes and a polyimide matrix has been reported by Gibbons et al.³⁵ Azobenzene molecular species, with transition moments (azobenzene $\pi-\pi^*$ transition) parallel to the polarization of the irradiated light (actinic light) underwent *trans-cis-trans (E-Z-E)* photochemical conversion in the blend film. The final in-plane projection resulted in a perpendicular orientation of the *E*-isomer with respect to the polarization, θ of the irradiated light (or parallel to the electric vector). This photoalignment has been consistently observed and demonstrated successively and selectively in a number of ultrathin film configurations: Langmuir monolayers, SAMs, LB multilayers, etc. This process is also found to be dependent on light intensity and irradiation time.³⁶

LBL Dye/Polycation Photoalignment. In this case, layer-by-layer ordered ultrathin films of water-soluble azobenzene dyes have been investigated. Figure 5a shows the UV-visible spectra of a polarized irradiated 50-layer film of PDDA/DR80 on a glass substrate from 10 to 100

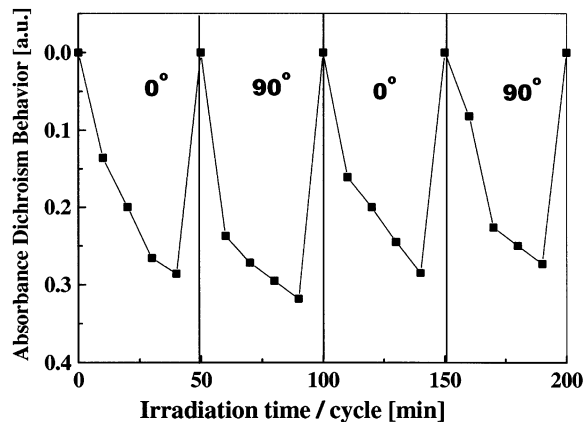


Figure 6. Cyclic photoalignment for the 50-pair-layer film up to four cycles. The absorbance at $\theta = 0^\circ$ decreases with time but becomes maximum at $\theta = 90^\circ$.

min of irradiation time.¹⁸ Prior to irradiation, the absorption is isotropic ($A_0 = A_{\parallel} = A_{\perp}$). The absorbance centered at 550 nm *decreases* as the film is exposed to parallel polarized irradiated light set at $\theta = 0^\circ$, giving the parallel absorption (A_{\parallel}). After the irradiation process at 0° , the substrate is then rotated 90° (perpendicular polarization direction) and the UV-vis spectra taken. Immediately a large difference in the absorbance is observed between 0° and 90° , indicating an increase in the population of absorbing species (dipole transition moment) to 90° or perpendicular to the original polarization of irradiated light as shown in Figure 5b. Again, this dipole orientation corresponds to azobenzene absorption behavior. The absorption band (A_{\parallel}) at 550 nm decreases with the irradiated polarized light since the absorbing azobenzene dye photostationary states at this orientation are depleted and become perpendicularly oriented giving rise to a higher perpendicular absorption (A_{\perp}). In this manner, a high dichroism was observed with DR = 0.4. Again, since the photostationary states under this illumination condition consist of the majority *E*-isomer, dichroism should be ascribed mostly to the long axis of the oriented chromophores. Our photoisomerization experiments *without* the polarizer gave no dichroism for these films. Furthermore, after irradiation, the unpolarized absorbance, A_{unpol} , also decreased, indicating partial reorientation of the chromophores into the S_z direction, leading to an increase in the orientation angle, α (see Figure 4).

Cyclic or reversible photoalignment was also investigated for the 50 pair-layer film. Figure 6 shows the photoisomerization process up to four cycles. It is clear that the absorbance shifts with polarization reversibly. Distinct photoselection in the absorption spectra is observed only when the film is irradiated for longer time periods, e.g. greater than 60 min. Shorter irradiation periods gave lower dichroic ratios. These observations are consistent with previously observed irradiation-dependent photoisomerization kinetics of LBL films.³¹ As shown in Figure 6, a clear decrease of the $\pi-\pi^*$ band was detected along the polarization direction (A_{\parallel}), which resulted to an enhanced absorption on the perpendicular state (A_{\perp}). Again, this was observed when the substrate is rotated from 0° to 90° with respect to the polarization setup of the UV-vis spectroscopy experiment. A slight decrease is observed at the fourth cycle. It could be related to the increasing fraction of azobenzene dyes that are becoming out of plane, S_z , from the substrate with successive irradiation.³⁴ It could also mean increasing steric restriction on the

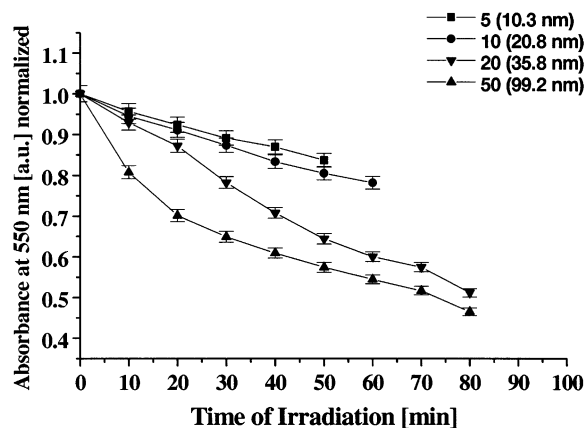


Figure 7. Photoalignment absorbance properties with different thicknesses of DR80/PDDA films: 5, 10, 15, and 20 pair-layers. A change in kinetics is observed beginning at 20 layers.

reforming aggregates. Nevertheless, a reversible cyclic photoalignment process was clearly demonstrated in these films.

As shown in Figure 7, the kinetics of absorption with photoalignment is also a function of thickness.³¹ The change in slope is evident on the kinetics plot for different thicknesses. Primarily, thicker films started to show two regimes (change in slope indicating a k_1 and k_2 process) with photoalignment.^{9,34,36} The kinetics of optical anisotropy in films consists of a fast and slow process: axis-selective photoselection involving $E-Z-E$ photoisomerization and subsequent photoreorientation of the molecular axis. The second process can take place very slowly in a glassy state, when compared with the first one, because the sweep volume required for the rearrangement of a rod-shaped molecular axis is much larger than that for the photoisomerization.^{9,36} Thickness dependence on photoisomerization has been reported previously for LBL films,³¹ where the extent of dye aggregation and layer ordering plays an important role. Thicker films have a higher total amount of azobenzene dyes and should result in more aggregated domains. Collectively, photoalignment, becomes a function of the total film thickness, where each layer contributes a finite number of photoaligning domains.³¹

The yield of the oriented photostationary E -isomer can be estimated by the decrease in the absorbance of the $\pi-\pi^*$ transition band during irradiation.³⁴ The kinetics can be modeled after the equation: $[E_t]/[E_0] = F \exp(-k_1 t) + (1 - F) \exp(-k_2 t)$, where the concentrations of the oriented photostationary E -isomer at time t and zero can be determined. F is the fraction of the fast species, and k_1 and k_2 denote the rate constants for the fast and slow processes, respectively. Consequently, more dye aggregates result in a larger initial $E-Z-E$ photoisomerization or faster k_1 . This is then followed by a slower reorientation, k_2 , of the azobenzene molecular axis with time.^{9,28}

Clearly, the differences of photochromism with different thicknesses are also due to matrix effects.² This matrix effect has two meanings: the effect of the matrix on the photochromic behavior and the effect of the photochromic behavior on the matrix. In the former, efficiencies of photochromism are affected by the microenvironmental properties of matrixes, including polarity, free volume, and molecule-to-molecule interactions, etc. The latter effect involves reversible property changes on matrixes as a result of structural transformation of photochromic guest molecules, leading to orientational alteration of host

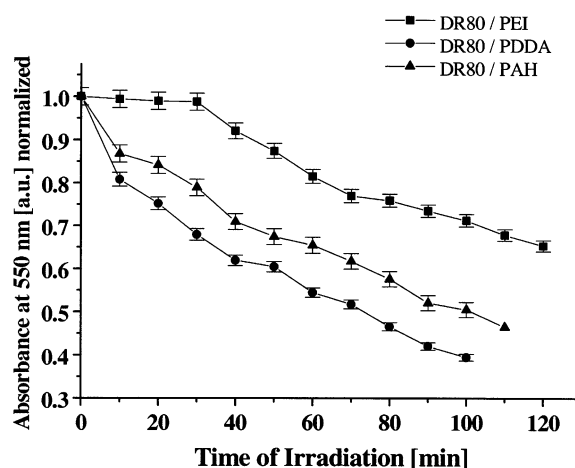


Figure 8. Photoalignment absorbance properties of DR80 paired with different polycation LBL films.

molecules or residues embedded in matrixes, which surround the guests. In principle, the orientational changes of matrixes triggered by photochromic molecules should be a useful probe for the physical as well as chemical condition of matrixes.³⁷

Figure 8 shows the photoalignment absorbance behavior with different polycation pairs at approximately the same thickness (60 layers). Different photoalignment kinetics can be observed, depending on the polycation used.³¹ As discussed earlier, PDDA showed the typical slope change associated with photoalignment kinetics up to the 100 min regime.³⁴ The PAH showed an almost similar behavior but with less absorbance change than in PDDA. The PEI showed a slow initial absorption change at the first 30 min followed by the change in slope. Previous studies have shown that DR80 with PAH and PDDA polycations have different aggregation behavior.¹⁸ The PAH is a linear polymer which has less cationic charges and is pH dependent. On the other hand, PDDA is a more linear polymer with a higher hydrophobic than ionic component. It is pH independent and has a higher MW. LBL films of dyes with PEI are typically more disordered with high interlayer penetration.^{16a,31} The presence of chain branching in PEI results in higher charge density that is pH dependent where desorption in LBL films has been reported.^{16a,31a} In general, the films prepared by PDDA compared to PAH and PEI are more uniform where the aggregates are well-defined.^{16,31} It seems reasonable to conclude that the kinetic behavior of PDDA films is influenced by the formation of more uniform DR80 aggregates in each deposited layer. Thus, for these LBL systems, the photoalignment behavior can be classified as a collective effect of well-defined aggregates that can be quantified by the number of layers and type of polycations used.

To contrast layer ordering in LBL films with isotropically distributed aggregates in spin-coated films, we compared their photoalignment behavior. The photoalignment behavior for DR80:PDDA films spin-coated (1500 rpm) from 1:1 polyelectrolyte complexes (PEC), 2% (w/w) dimethylacetamide (DMAC) or aqueous solutions, are shown in Figure 9. Ultrathin films were formed which have thicknesses measurable by ellipsometry. In general, the films are not as uniform (optically) compared to polymer films commonly spin-cast from organic solutions. Depending on the thickness of the spin-coated films, different photoalignment kinetics can be observed. The spin-coated films of comparable thickness (105 nm) to the LBL (110 nm) showed a slower kinetics behavior with a

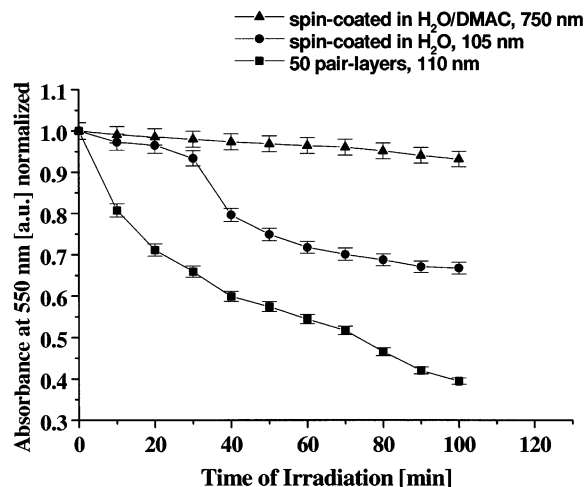


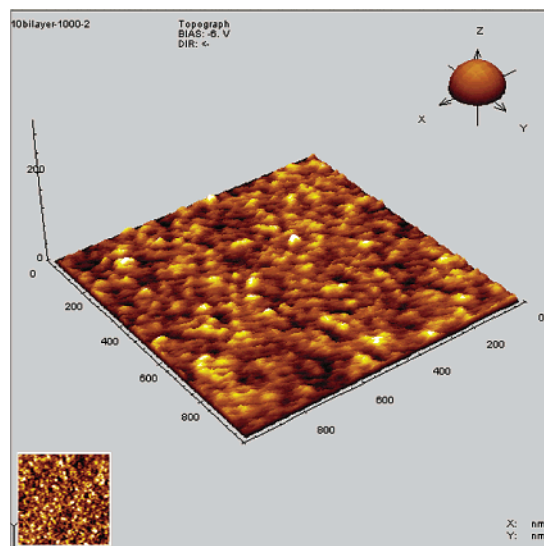
Figure 9. Photoalignment absorbance properties of DR80 and PDDA as spin-coated films in comparison with LBL films.

slope change at 30 min followed by a monotonic plateau behavior. This curve is not reproducible and was dependent on film quality. Furthermore, thicker layers (750 nm) of the PEC films did not show significant change in absorption with time. No well-defined cyclic reversible photoalignment behavior was observed with the spin-coated films. It should be noted that these spin-cast films were prepared from a binary polyelectrolyte complex. Uniform films require some experimentation with rotation speed and solvent conditions (different concentrations or mixtures). In fact, one of the advantages of the LBL technique is that ultrathin films can be formed on substrates, which often has no equivalent to spin-coatable solutions.

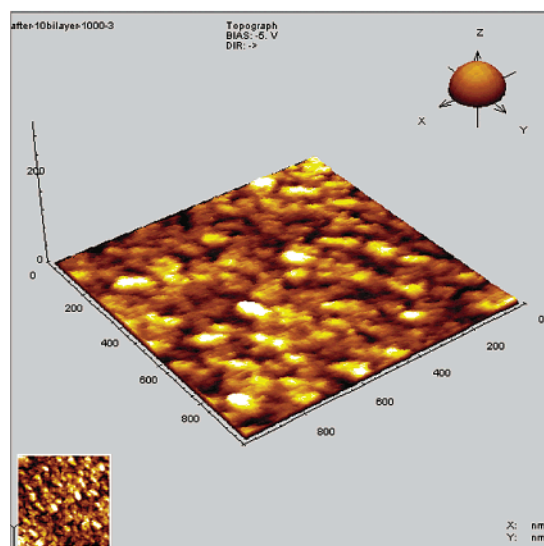
AFM Images. AFM images before and after UV irradiation give further insight into the photoisomerization and photoalignment process with these films.³⁸ Figure 10 shows micrographs of the DR80/PDDA films with various layer thicknesses. The morphology is comprised of corrugated features with depression and ridges. Although it cannot be directly imaged by AFM, these features comprise a *distribution* of dye aggregates of undetermined size and number.³⁸ The roughness and feature size is observed to change with increasing thickness. Thicker layers tend to produce larger feature sizes with increased roughness. This behavior correlates with some of the photoisomerization behavior observed and the fact that the λ_{\max} shifts with different thickness (Figure 3).

Also shown are micrographs of the 30 pair-layer films before (Figure 11a) and after 2 h irradiation with unpolarized (Figure 11b) and polarized (Figure 11c) visible light > 430 nm. First of all, after irradiation, all of the corrugated features enlarged regardless of the polarization state of light. In particular, irradiation with unpolarized light resulted in a slightly smoother film (lower root mean square roughness ~ 3.9 nm) with larger feature sizes. It is well-known, the *trans*-*cis* photoisomerization causes an increase in the area per molecule in LB films due to the change in molecular configuration.⁹ Expansion of the features indicates the occurrence of photoisomerization in these films where the *trans*-*cis*-*trans* photoisomerization is induced. This phenomenon has been observed on a number of AFM-photoisomerization experiments in monolayer films.³⁸

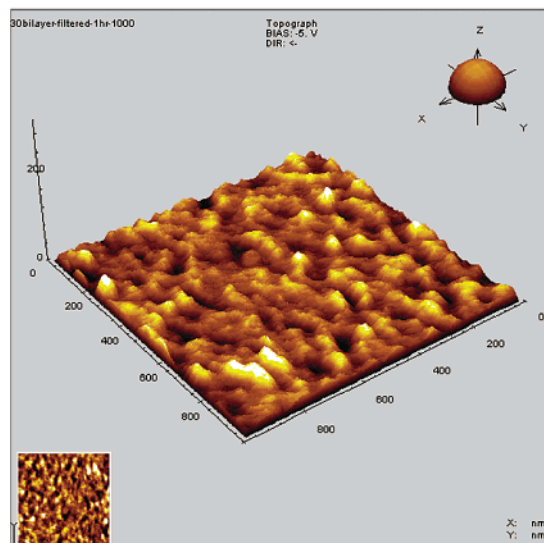
When polarized visible irradiation was applied to the film (Figure 11c), with the electric field parallel to the longer side of the substrate, the features showed a distinctly different behavior. As determined from these



1 -pair-layer (0.9 nm r.m.s)



10- pair layers (2.2 nm r.m.s)



30 -pair layers (4.6 nm r.m.s)

Figure 10. AFM images of the films: Morphology of the DR80/PDDA at various thicknesses (X - Y - $Z = 1.0 \times 1.0 \times 0.25 \mu\text{m}$ scans).

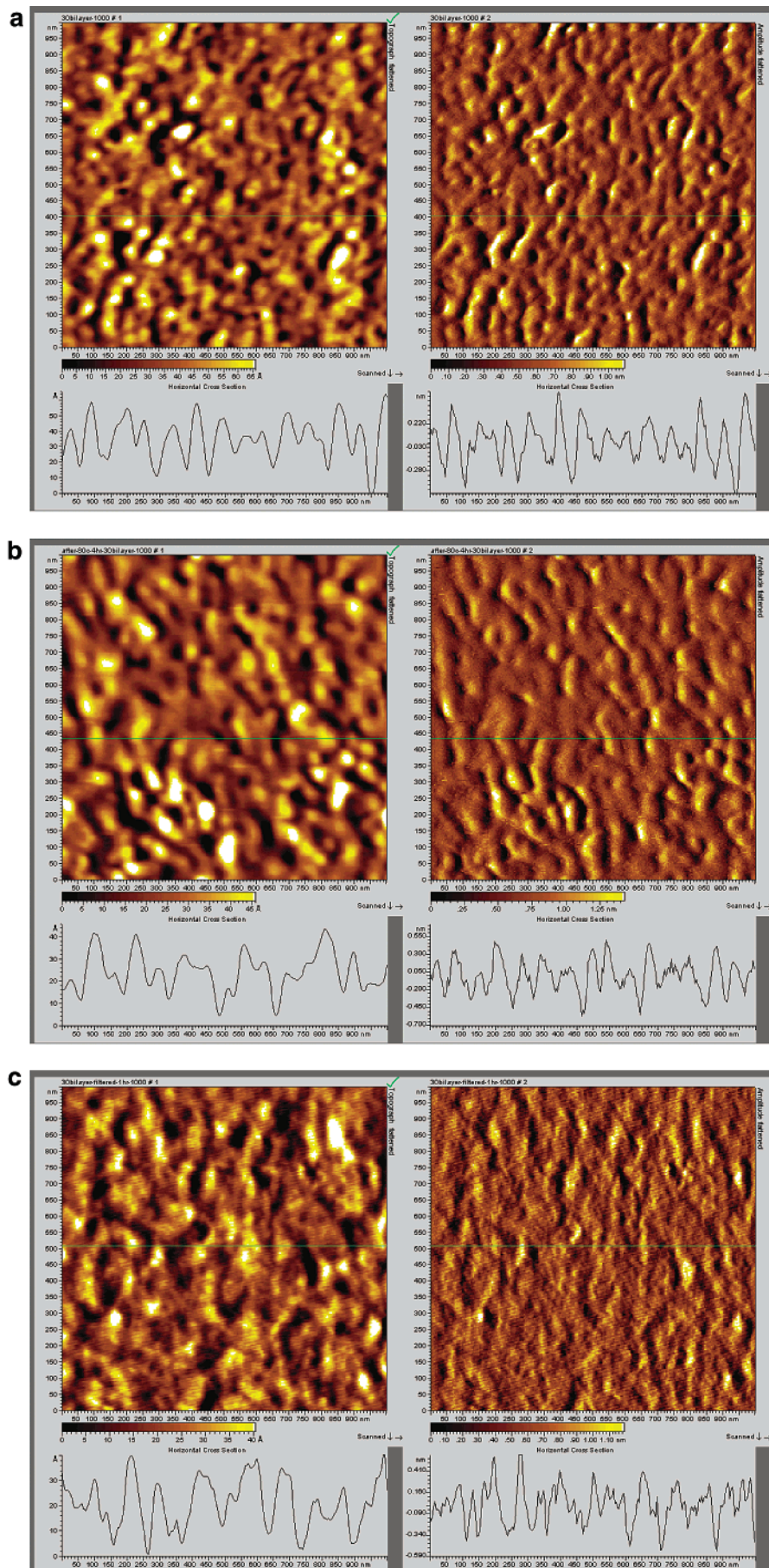


Figure 11. AFM images of the films: (a) before irradiation (4.6 nm; $X-Y-Z = 1.0 \times 1.0 \times 0.05 \mu\text{m}$), (b) after 2 h unpolarized irradiation (4.1 nm rms; $X-Y-Z = 1.0 \times 1.0 \times 0.05 \mu\text{m}$), and (c) after polarized irradiation for 2 h (3.8 nm rms; $X-Y-Z = 1.0 \times 1.0 \times 0.05 \mu\text{m}$).

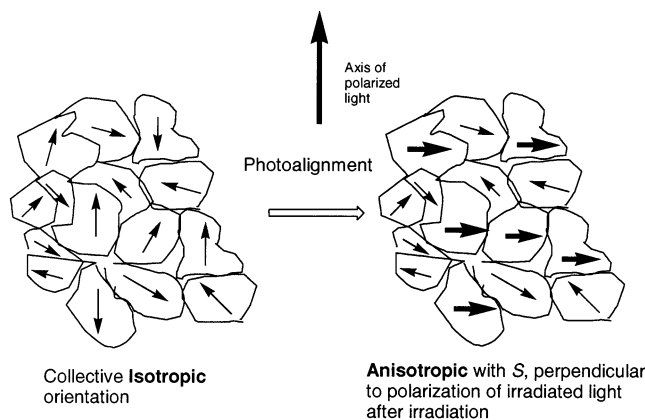


Figure 12. Schematic diagram showing change in the collective isotropic orientation of the dye aggregates and the photoalignment of individual domain aggregates after polarized irradiation. Note the orthogonal nature of the dye orientation with respect to polarized light axis.

images, after polarized irradiation, the ridges in some regions not only expanded in area but also became slightly elongated and sharp. This comparison is evident especially on the FT-phase images (right side), where the textures are different. These observations correlate with the selective photoisomerization observed.

The phenomena of aggregate growth and orientation in morphological features before and after photoisomerization have been previously studied.^{34,38} The following mechanism has been described (Figure 12): A large domain or feature might be composed of a *distribution* of smaller oriented aggregates (subdomains) in individual directions. The transition moments of the chromophores within these individual smaller aggregates, based on the in-plane projections of the molecules, are presumed to point in approximately the same direction with a director, S .³⁴ The in-plane transition moment projection in neighboring aggregates should also have an oriented average direction. The result is that the initial unirradiated film should have an overall isotropic orientation based on a collective orientation of all the smaller aggregates.³⁹ By irradiation with only unpolarized light, no selective reorientation is expected but only a reorganization of the domains toward greater "swift volume" because of successive trans-cis-trans photoisomerization.^{34,36} This is similar to thermal annealing for these films where smoother films are generated, decreasing kinetically trapped conformations and aggregates of the dyes formed during the deposition process. The observations in Figure 11b are consistent with this mechanism.

The situation with polarized light is different (Figure 11c). Aggregates with in-plane transition moment projections parallel to the polarization of irradiated light will be subject to selective trans-cis-trans photoisomerization. This is because aggregated azobenzene molecules occur as ordered structures, with a strong cohesive energy where each domain is relatively independent of the neighboring domains.^{34,38} Aggregates with uncorrelated orientations with respect to the polarized irradiation will be scarcely influenced. However, aggregates with their molecular orientations in the polarization direction of irradiated light will show significant enlargement in size because of anisotropic reorientation (Figure 12). This behavior is indicative of a photoselection process, where the collective aggregates (resulting morphological features) showed a relatively large degree of expansion, whereas others maintained their individual sizes after irradiation (comparison of Figure 11b,c). This supports

the notion that dye aggregates can be regarded as a "photoreacting units" consistent with those observed in other types of azobenzene containing films.^{34,38} The average excitation probability within these units depends on the director orientation: $P_{\text{exc}} \propto (V_E \mu_t)^2$, where μ_t is the azobenzene electric dipole transition moment and V_E is the irradiation electric field. The effective irradiation intensity needed to reorient these aggregates is given by $I_{\text{eff}} = I_0 \cos^2 \varphi$, where φ is the azimuthal angle between μ_t and V_E (Figure 4). I_{eff} must exceed the intensity threshold, I_{th} , for reorientation of the aggregates to occur.³⁴ Thus, the AFM images acquired with different irradiation conditions on either unpolarized or polarized light are consistent with this mechanism. A detailed study comparing the mechanism of photoalignment with SAM and LB films should be interesting.

Hybrid LC Cell Studies. *In-Plane Photoalignment.* Hybrid LC cells were fabricated by sandwiching a nematic LC (5CB) between the DR80/PDDA films and a glass substrate modified with a stearic acid monolayer for homeotropic alignment on one side (Figure 2).⁴⁰ The cells were irradiated with linearly polarized visible light (> 430 nm) normal to the substrate plane, for $n-\pi^*$ excitation. The $n-\pi^*$ excitation with linearly polarized visible light causes azimuthal reorientation of the LCs primarily through the reorientation of the E -photostationary state of the azobenzene aggregates. The rodlike-shaped E -isomer of the chromophore plays an essential role in the in-plane homogeneous alignment regulation as a "molecular rotor".^{9,10,11}

For the experiments, the polarization plane of actinic light at $\theta = 0$ is parallel to the longer side of the rectangular cell, as illustrated in Figure 2. The birefringence was monitored by following the intensity of transmitted linearly polarized He-Ne laser beam through the cell and a fixed polarizer (analyzer) position.²⁸ The experiment is essentially a cross-polarizer experiment, where the transmission is monitored as a function of the rotation angle (ϕ) of the cell.

The polar plot in Figure 13a shows the evolution of transmittance with time as monitored through the cell. The cell was rotated at an angle ϕ . For a 100 pair-layer of DR80/PDDA film the first few minutes did not produce significant changes in the transmission-angle dependence. However, at 45 min the birefringence began to be observed and was fully developed at 60 min. The maximum transmittances are approximately located at $45^\circ \pm 90^\circ \times n$, indicating the director (S) of the LC molecules exists perpendicular to the polarization plane. The maximum of transmittances is reached at 80% after 60-min irradiation and finally at 90% after 120-min irradiation (not shown). The angular dependence of transmittance of the monitoring light for a hybrid LC cell with a 10 pair layer DR80/PDDA was also examined (data not shown). It was found that the maximum transmittance was about 80% (after 10 min), where the process of alignment of LC was faster than that of a 100 bilayer DR80/PDDA cell. These results are consistent with the photoalignment behavior as observed with the DR80/PDDA films using polarized UV-vis spectroscopy. In previous studies, the kinetics of photoisomerization of LBL films was influenced by the thickness of the samples; i.e., the isomerization is slower for the thicker samples.³¹ Since the homogeneous alignment of LC molecules is controlled by the photorientation of azobenzenes in DR80/PDDA films, it is clear that the kinetics of alignment of LC molecules can be influenced by the *thickness* of DR80/PDDA film. This indicates that LC reorientation may not simply be a function of the immediate azobenzene-polyelectrolyte layer in contact

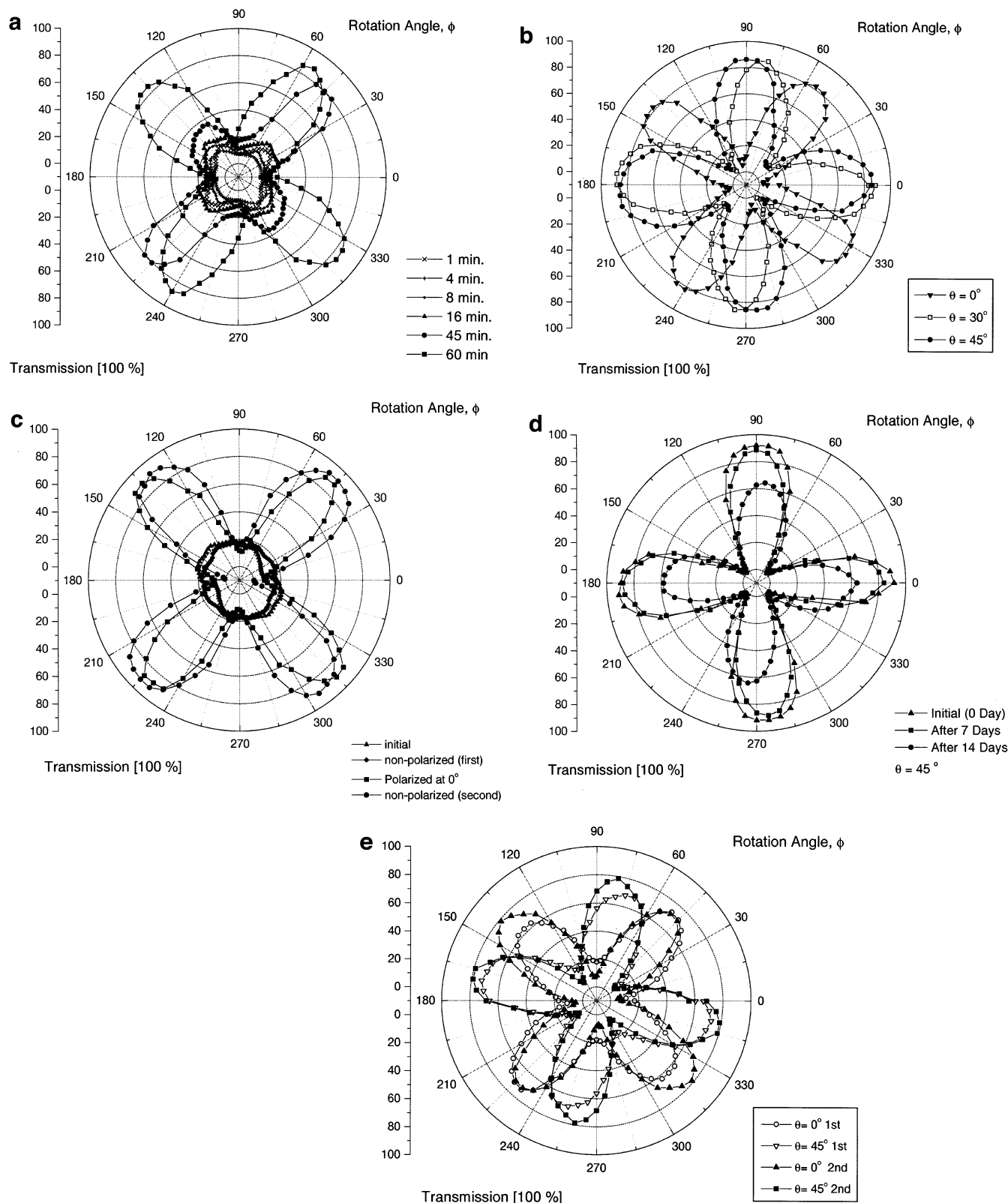


Figure 13. (a) Time-dependent in-plane photoalignment behavior for a 100 pair-layer of DR80/PDDA. (b) Phase shift with respect to angle of irradiated light for a 50 pair-layer of DR80/PDDA. (c) Stability of photoalignment with polarized and unpolarized irradiation for a 100 pair-layer of DR80/PDDA. (d) Stability of photoalignment with time for a 100 pair-layer of DR80/PDDA. (e) Read-write capability for a 10 pair-layer of DR80/PDDA.

with the LC molecules, but may be influenced by the overall thickness, layer ordering, and morphology of these films. This is in contrast to previously reported photoalignment behavior in LB and SAM films which is thickness independent.^{9–11} It is well-known that dipole forces, polarity, surface energy, and topological factors

influence the surface anchoring energy of LC molecules⁴¹ and has been modeled.⁴² It will be important to do careful

(41) de Gennes, P. G.; Prost, J. *The Physics of Liquid Crystals*; Clarendon Press: Oxford, U.K., 1993. (42) Chandrasekhar, S. *Liquid Crystals*, 2nd ed.; Cambridge University Press: Oxford, U.K., 1992.

fundamental studies on the differences in a “command-layer” effect on LBL films compared to LB and SAM films.

Phase Shift. To examine photoalignment control of the LC molecules further, we irradiated uniformly preirradiated cells by linearly polarized light at various axes. Figure 13b shows the *shift* of the transmittance curve as a function of irradiation angle from $\theta = 0^\circ$, 30° , and 45° after irradiation with the actinic visible light (> 430 nm) at various axes. The transmittance maximum appears periodically at $\theta + \pi/4 + \pi/2 \times n$ ($n = \text{integral numbers}$), confirming a homogeneous alignment perpendicular to the polarization plane of the irradiation light. It is clearly shown that the direction of in-plane alignment can be controlled by the angle, θ , of the linearly polarized light, resulting primarily in a *phase shift* of the transmittance curve.

Stability. The stability of the LC cell was examined. The LC cell was first exposed to unpolarized light for up to 60 min (Figure 13c). No photoalignment was observed. Upon applying polarized light, the typical birefringence change in transmittance was observed. The cell was then re-irradiated with unpolarized light. The birefringent transmittance behavior barely changed. This indicates the stability of the original photoalignment against unpolarized irradiation fields, indicating that apart from selective photoisomerization, the dyes are expected to keep their molecular long-axis orientation. These observations are also consistent with the AFM results.

Also the film was left for 2 weeks under ambient conditions (room temperature and exposed to air), and the transmittance was monitored as a function of time (Figure 13d). A slight decrease in intensity was observed after 1 week. However, after the second week, a larger decrease in intensity was observed but with the photoalignment orientation hardly changed. Our results with a 10-layer film (not shown) gave a faster decrease in transmittance and birefringence loss to within days. Thus, photoalignment stability is also related to film thickness. This is consistent with thickness-dependent photoalignment behavior during the original irradiation.

These results clearly show that stability of the original LC alignment toward maintaining high anisotropy. The use of unpolarized light did not result in any optical birefringence of the transmission once photoalignment has been achieved. Furthermore, it should be possible to use a selective cutoff filter, which decreases the amount of *E*-isomers, which could result in the loss of the birefringence transmission properties.

Read-Write Capabilities. To demonstrate read-write capabilities, the cell was initially irradiated uniformly with one orientation and re-irradiated to another linearly polarized light angle and back again. Before the experiment, the cell was preirradiated with linearly polarized light at $\theta = 0^\circ$ for 60 min. Figure 13e shows the *shift* of transmittance when the cell was subsequently irradiated with linearly polarized light with the polarization plane at $\theta = 0^\circ$ and then at 45° . After 90 min of irradiation, the full transformation of the molecular axis of the azobenzene to perpendicular to the electric vector of the second light was achieved. This was then repeated for a second cycle between $\theta = 0^\circ$ and 45° . Again, for both

cycles, the transmittance maxima appears $\theta + \pi/4 + \pi/2$, confirming a homogeneous alignment perpendicular to the polarization plane of the irradiation light. Note that the second cycle resulted in a higher transmittance and with no hysteresis. The birefringence seemed to have been improved on the second cycle after the creation of a larger swift volume for the dye to reorient with light. It is clear that the direction of in-plane alignment changed with θ reversibly for the 10-layer film. But for the 100-layer thick films (data not shown) at 60 min irradiation time, this resulted in some hysteresis behavior, again confirming a thickness-dependent photoalignment behavior.

Overall, the LC photoalignment behavior is found to be distinct for LBL films in contrast to SAM monolayers and LB films,^{9–11} where the immediate monolayer largely influences the LC alignment behavior. We have recently reported in-situ attenuated total reflection (ATR) measurements to investigate the layer ordering and LC alignment in hybrid LC films with a Kretschman optical configuration⁴³ as well as holographic surface relief grating formation⁴⁴ on these films. Selective photoalignment with the use of a patterned mask should be possible.

Conclusion

In this paper we have described the formation and photoinduced alignment of layer-by-layer deposited ultrathin films of a small molecule azobenzene dye (direct red 80) and polycations using the alternate LBL adsorption technique. The water-soluble chromophoric dye with a high aspect ratio *E*-isomer functions as a molecular rotor. The photoalignment studies on the DR80/polycation pairs were found to have high anisotropies after irradiation with linear polarized visible light. Correlation was made on the effect of film thickness, polycation pair, and comparison to spin-coated films. Layer ordering, dye aggregation behavior, and topological structures were found to be important to their photoalignment properties. Optical retardation in hybrid LC cells was observed as a function of polarizer-analyzer angle. In-plane selectivity of the photoisomerization process was found to be associated with the aggregation nature of the domains in the film, film thickness, irradiation time (and intensity) resulting in the reorientation of the LC molecules. Photoalignment reversibility was observed offering the potential for read-write capabilities. Thus, the incorporation of a photochromic moiety using the LBL technique is very attractive for creating new light-sensitive optical materials and devices from polyelectrolyte materials and water-soluble dyes.

Acknowledgment. We thank Keizo Kato and Kazunari Shinbo of Niigata University, Eric Fells, and Yingfan Wang for helpful discussions. Funding from ACS-PRF, PRF-35036-G7 and technical support from Molecular Imaging Inc. and Optrel GmbH are gratefully acknowledged.

LA025842L

(43) Ishikawa, J.; Baba, A.; Kaneko, F.; Advincula, R.; Shinbo, K.; Kato, K. *Colloids Surf., B* **2002**, *198–200*, 917.

(44) Katowa, T.; Baba, A.; Kaneko, F.; Advincula, R.; Shinbo, K.; Kato, K. *Colloids Surf., B* **2002**, *198–200*, 805.

(42) Palto, S.; Barberi, R.; Iovane, M.; Lazarev, V.; Blinov, L. *Mol. Mater.* **1999**, *11* 277.